applied sciences

MDPI

Article

Performance-Based Fibre Design for Ultra-High Performance Concrete (UHPC)

Jan-Paul Lanwer * and Martin Empelmann

iBMB (Institute of Building Materials, Concrete Construction and Fire Safety), Division of Concrete Construction, TU Braunschweig, 38106 Braunschweig, Germany
* Correspondence: j.lanwer@ibmb.tu-braunschweig.de

Abstract: The paper presents a method to establish a performance-based fibre design of high-strength micro steel fibres for ultra-high-performance concrete (UHPC). The performance-based fibre design considers effects of fibre layout, fibre orientation, and type of loading (quasi-static and cyclic) and expands the current approach using experiences and suitability testing results. The performance-based fibre design is based on a so-called utilization rate, which is determined via pullout tests of high-strength micro steel fibres in UHPC under quasi-static as well as high cyclic loading with varying orientations and embedment depths. The utilization rate for a straight fibre pullout is 0.27 on average considering the measured tensile strength of the fibre and 0.50 considering the manufacturers specifications. For inclined fibres, additional bending stresses occur at the exit point of the fibre channels, leading to a significant increase in local tensile stress. Therefore, the utilization rate of inclined fibres under quasi-static loading is approximately 60–70% higher than in the case of straight embedded fibres (comparing it to the measured tensile strength). Comparing the utilization rate to the manufacturer's specification, it increases to approximately 1.00. Under cyclic loading, the additional bending stresses in inclined fibres result in a local increase of the load amplitude, leading to a reduced fatigue resistance and premature fibre rupture, underlining the feasibility of a performance-based fibre design.

Keywords: ultra-high performance concrete (UHPC); fatigue; fibre pullout; fibre rupture; fibre design

Citation: Lanwer, J.-P.; Empelmann, M. Performance-Based Fibre Design for Ultra-High Performance Concrete (UHPC). *Appl. Sci.* **2022**, *12*, 8559. https://doi.org/10.3390/app12178559

Academic Editor: Chao-Wei Tang

Received: 10 June 2022
Accepted: 24 August 2022
Published: 26 August 2022

1. Introduction

The high fibre content in ultra-high performance concrete (UHPC) provides a positive ductility under compressive loading and a considerable post-cracking tensile strength under tensile loading. Because of the increasing importance of resource conservation, it is no longer appropriate to allow "unused capacities" in building materials. Taking into account the obliged performance, the best way to prevent unused capacities is the optimal utilisation of the mechanical properties, such as e.g., the post-cracking tensile strength. The level of post-cracking tensile strength directly links to the fibre content and the fibre design. The fibre design, in turn, comprises the choice of the fibre material and fibre geometry as well as the fibre tensile strength.

Empirical values, experiences, and suitability tests are often the current practice in regards to selecting a fibre type for fibre reinforced concrete members. They all have little mechanical background and do not consider complex load scenarios. Therefore, fibre design in terms of an optimal application to the performance requirements should explore for new methods.

This paper demonstrates a mechanical approach for a performance-based fibre design of high-strength micro steel fibres for UHPC. Besides experiences in fibre design, the novel approach intends to cover the effects of fibre orientation and cyclic loading in addition to empirical values and suitability tests. The novelty of the approach is the gained knowledge of the fibre stresses in tensioned UHPFRC. Until now, it has remained largely

unclear how fibres are utilised in cracked UHPFRC, i.e., it might be possible that the fibre stresses are close to fibre rupture or relatively low so that the fibre design is inefficient. Especially inclined fibres (compared to the direction of loading) face completely other stress distributions as straight fibres. These stress distributions have a great influence in the fibre design. The novel approach considers the stresses that occur from the oblique position of the fibres and shows, e.g., the reserves of a UHPFRC-component against failure. Furthermore, and besides static loading, it is unknown how inclined fibres respond to cyclic stresses. The approach tries to give information on the maximum applicable stresses for fibres under cyclic loading in UHPFRC.

The basis of the approach rests upon pullout tests of high-strength micro steel fibres from UHPC with different orientations and embedded lengths carried out under quasi-static as well as cyclic loading at iBMB, Division of Concrete Construction, TU Braunschweig.

2. State of the Art of Fibre Design

The intended softening respectively ductile material behaviour of fibre concretes can only be achieved, if the tested fibre design leads to fibre pullout instead of fibre rupture [1,2]. Therefore, the fibres have to match to the strength properties of the concrete. Not all fibre types are in the same way suitable for each concrete type. This means, for example, that valuable high-strength micro steel fibres are much more suitable for concretes with higher strengths like UHPC [3,4] and conventional hooked macro fibres are suitable for normal performance concrete (NPC). Studies on fibre pullout in high- and ultra-high performance concrete were carried out, e.g., in [5–10].

Jungwirth [5] points out that inclined embedded steel fibres exhibit higher pullout resistances compared to straight embedded fibres. The deflection of the fibre at the exit point of the fibre channel, where the fibre rubs against the wall, results in high frictional and therefore higher pullout forces. However, it might also be possible that inclined fibres cause spalling of concrete fragments at the edges to the main crack, which then reduce the rubbing and bending effects. In addition, high amounts of fibres in concrete lead to a very close fibre location and mechanical interaction of fibres in components might be expected.

Rieger [6] investigates the dependence of the pullout resistance of micro steel fibres on the water-cement ratio (w/c ratio) and the embedment depth. A high w/c ratio leads to a higher porosity in the bond zone and lowers the pullout resistance, whereas a higher embedment depth increases the pullout resistance. In all carried out pullout tests the fibre pullout was always initiated under quasi-static loading.

Stengel [7] states that pullout forces of inclined fibres are 1.8–2.7 times higher, compared to a straight fibre pullout. In addition, fibre rupture occurred in the pullout tests for fibres with a mechanical end anchorage. On the other hand, no fibre rupture was observed in pullout tests with straight fibres and no end anchorage.

Refs. [8–10] contain fibre pullout test of high-strength steel fibres without mechanical anchorage in ultra-high-performance concrete. In all studies, continuous fibre pullout took place, which means that the activated bond stresses did not exceed the tensile strength of the fibre material. Furthermore, [10] includes pullout tests of individual fibres and fibre groups with different orientations. Similar to [5], concrete breakout at the fibre exit point was observed affecting the mechanical properties.

In all the aforementioned works, no fibre rupture occurred under quasi-static loading, unless the fibres have a mechanical anchorage. However, the literature review does not clarify what happens with embedded fibres under cyclic loading. It could be possible that the fatigue resistance of the bare fibre material is higher than the fatigue resistance of the bond zone between fibre and concrete or vice versa. This might lead to either fibre rupture or fibre pullout.

Results of investigations on the load-bearing behaviour of UHPC components with a 3D-fibre distribution under cyclic tensile loading are partly available, however, they are mainly limited to the derivation of S/N-curves [11–13]. The findings of the investigations

leave the question unanswered, whether embedded fibres pull out of the concrete matrix or rupture in the crack area under cyclic loading.

3. Fibre Design Approaches

3.1. Conventional Approach

For normal strength steel fibre concrete, usually macro steel fibres are used, whose slenderness, i.e., the ratio of length to diameter, is about 60 [-]. The diameter of the common macro steel fibres varies between 0.50 mm and 1.20 mm and the length between 30.0 mm and 70.0 mm. The tensile strength of these macro steel fibres is about 1000 N/mm^2.

The tensile strength of the fibre material has roughly tripled in recent years, which makes them increasingly appropriate for high and ultra-high-performance concrete [14]. Figure 1 shows some steel fibre types for normal-, high- and ultra-high-strength concretes.

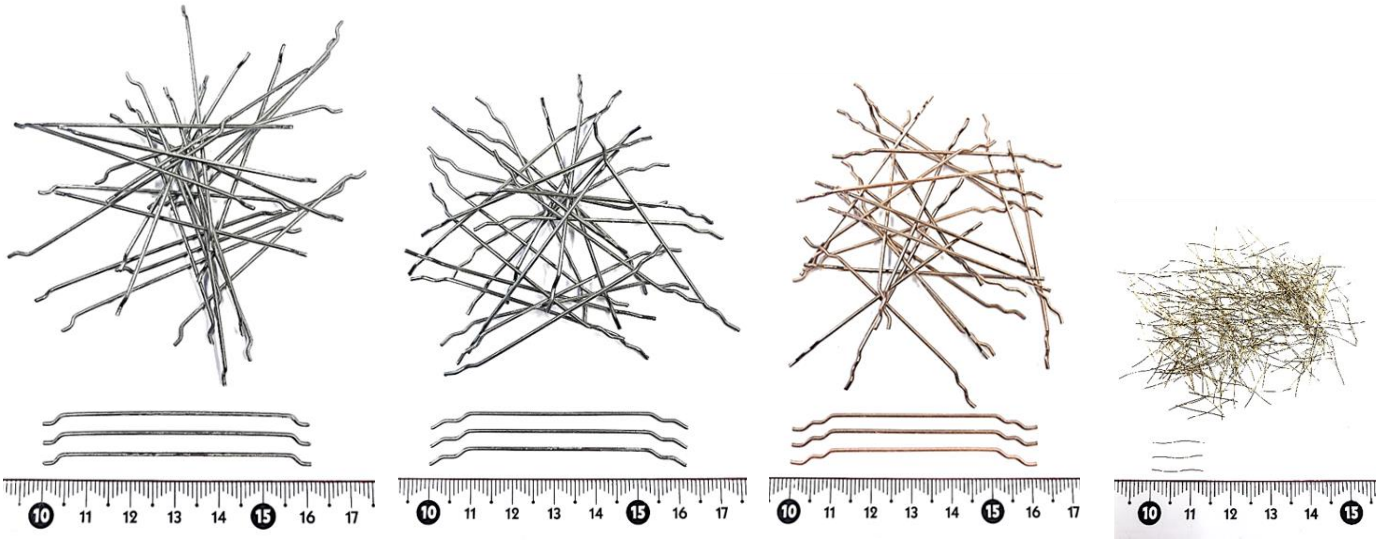

(**a**) (**b**) (**c**) (**d**)

Figure 1. Types of steel fibres for normal, high- and ultra-high performance concrete: (**a**) 3D-fibre (**b**) 4D-fibre (**c**) 5D-fibre and (**d**) high-strength micro steel fibre.

Due to the comparatively low bond stress of plain steel fibres in normal strength concrete, macro steel fibres usually have end hooks (anchorages) increasing the pullout resistance. The geometry (especially with regard to the end anchorage) and tensile strength of the fibres should be matched in such a way that continuing pullout occurs in steel fibre reinforced concrete components under tensile stress.

Macro steel fibres with mechanical anchorage are normally not suitable for high and ultra-high performance concrete. The high bond stress in addition to the anchorage force of the end hook would exceed the material strength of the fibres and thus causing an unwanted fibre rupture [7]. Therefore, plain high-strength micro steel fibres with diameter between 0.10 mm and 0.25 mm and length between 6.0 mm and 25 mm suit much better for UHPC. The tensile strength of such micro steel fibres is usually significantly more than 2000 N/mm^2.

Modern steel fibre types have an optimized anchorage (e.g., a second hook, cf. 5D-fibre in Figure 1c), leading to an intended fibre rupture under quasi-static loading. In that case, the elongation capacity of the steel fibre material defines the post-cracking tensile behaviour of the fibre concrete.

3.2. Novel Deterministic Approach

The aforementioned properties of the fibre material in connection with the surrounding concrete are based on empirical experiences and suitability tests and have large geometric ranges. Up to now, there is no deterministic procedure for establishing a purpose-oriented

respectively performance-oriented fibre design, which, in addition to the above, takes into account the effects of orientation and cyclic loading. Figure 2 shows a flow chart for establishing a method for a deterministic fibre design.

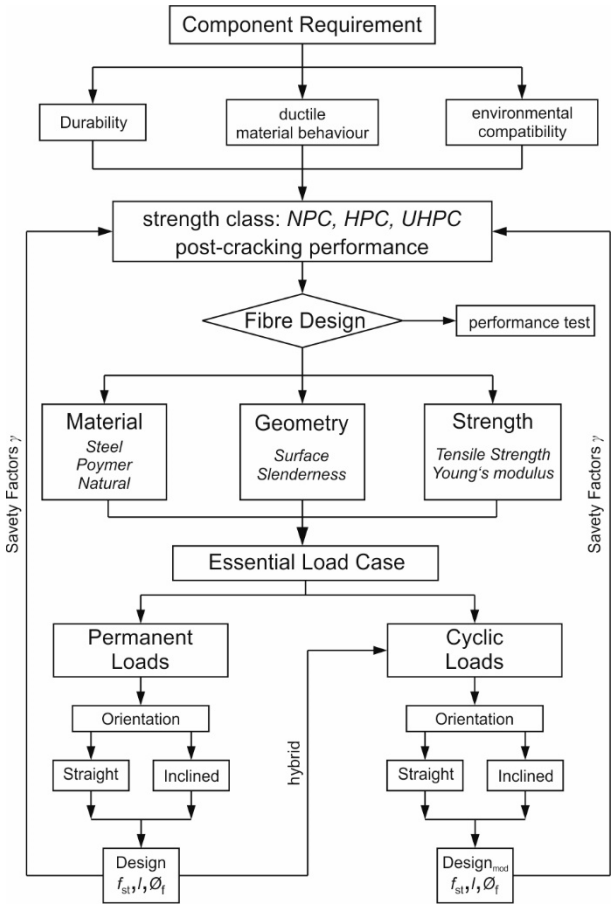

Figure 2. Flow chart for a deterministic fibre design.

The fibre design starts with a definition of the component requirements, e.g., the durability, load bearing capacity, and environmental compatibility. The requirements of the component normally determine the concrete strength class and the post-cracking tensile strength. Subsequently, the fibre design, i.e., the material, geometry and strength, are preselected based on empirical experiences and, if necessary, existing performance tests. As such preselection does not cover complex stress situations, further steps are necessary. So, the relevant load cases of the component must be figured out. If the component is mainly subjected to quasi-static loading, it is sufficient to assess the orientation and adapt the fibre design. However, if cyclic loading occurs, the fibre design requires an adjustment to the stress situation. Once the fibre design is classified, the fibre content can be determined via safety factors or safety margin.

The flow chart for a deterministic fibre design makes the application of fibres in fibre reinforced concrete structures more efficient. It gives the designer information in the form of a road map which fibres might be useful in the planned component. Therefore, the current empirical methods for the fibre design in UHPFRC might not be applicable anymore.

4. Experimental Investigation

4.1. High-Strength Micro Steel Fibre, Test Specimen and Test Programme

The experimental investigation was conducted with an ultra-high performance concrete, which has its origin in the DFG Priority Program 1182 [15], and a high-strength steel fibre. The mixture composition of the UHPC is listed in Table 1 and [16].

Table 1. Mix composition of UHPC.

Components	Amount
[-]	[kg/m^3]
Cement CEM I	795.0
Silica fume	168.6
Superplasticizer	24.1
Quartz powder	198.4
Quartz sand 0.125/0.50 [mm]	971.0
Water	189.9

In [17], the compressive and tensile material behaviour is described in detail. The compressive strength of the UHPC is approximately 149.2 N/mm^2 and the tensile strength is approximately 10.7 N/mm^2, both on average. The Young's modulus of the concrete material is approximately 43,300 N/mm^2. All material data come from a concrete age of more than 28 days.

The high-strength micro steel fibre is 13.0 mm in length and 0.19 mm in diameter. That gives a slenderness ratio according to Equation (1). The tensile strength is more than 2000 N/mm^2 and the Young's modulus around 200,000 N/mm^2, according to the manufacturer's data. The fibre surface has a brass coating.

$$l_f/\varnothing^f = 13.0/0.19\ [\text{mm/mm}] = 68. \quad (1)$$

Most investigations in the SPP1182 were limited to quasi-static loading, so that fundamental experiences on cyclic loaded ultra-high-performance fibre-reinforced concrete (UHPFRC) are missing. However, a comparable type of fibre has been used in fatigue exposed UHPFRC-structures [18].

The own experimental investigations on the pullout behaviour of high-strength micro steel fibres in ultra-high-performance concrete (UHPC) were carried out on single fibres (abbreviation: VES) as well as on groups of fibres (abbreviation: VMS). Refs. [1,16,17,19] contain detailed information of the test specimen configuration, fabrication, and execution of the pullout tests.

With the exception of the pullout tests with single fibres, the pullout tests were performed under both quasi-static as well as cyclic loading. For single fibres, cyclic loaded pullout tests were not possible due to a high scattering in the pullout behaviour and an impossible calculation of reliable load amplitude. The test program contained two different embedment depths of the fibres in UHPC, namely 3.25 mm and 6.50 mm. The orientation of the fibres was chosen to be 90°, 75°, 60°, 45°, and 30° with respect to the crack opening. The amplitude related to the static pullout force varied for the fibre group pullout tests between 0.15 and 0.75.

4.2. Investigation Results

4.2.1. Quasi-Static Loading

Table 2 shows a part of the test program and particularly the tensile stresses in the fibres that have been calculated back from the machine load. In the pullout tests of the fibre groups, nine fibres were pulled out of the UHPC simultaneously, with the load distributed uniformly to all nine fibres. The diameter of the tested fibres was assumed to be 0.19 mm according to the manufacturer's specifications and the studies in [1]. The load–displacement curves can be obtained from [19].

The "measured" embedment depths in Table 2 were determined using the linear variable differential transducer of the testing machine after all fibres were completely pulled out of the UHPC. The deviation of the actual measured embedment depth (also given in Table 2) from the intended embedment depth rests upon the high energy of the compaction process, which led to a partial slippage of the fibres in the UHPC formwork.

The utilization rate is related to the tensile strength of the high-strength micro steel fibre, which was determined in [1] to be $f_{st}^f = 3575.8$ N/mm^2, deviating significantly

from the manufacturer's specifications (2000 N/mm^2). The mean utilization rate for micro steel fibres in UHPC was determined as $\eta_{mv} = 0.27$, with all utilisation rates below 0.38, indicating a pullout failure in any case (cf. Figure 3).

Table 2. Test results, calculated tensile stresses and utilisation rate in relation to the fibre strength.

Series	Amount	Aimed Embedded Length l_e	Orientation Angle α	Measured Embedded Length $l_{e,m}$	Tensile Stress/ Fibre σ^f_{st}	Utilisation Rate $\eta = \sigma^f_{st}/f^f_{st}$
[-]	[-]	[mm]	[°]	[mm]	[N/mm^2]	[-]
VES30-1	3	3.25	30	3.11 ± 0.61	940.1 ± 528.1	0.26
VES30-2	3	6.50	30	6.87 ± 0.79	1329.5 ± 459.1	0.37
VES60-1	4	3.25	60	2.88 ± 0.11	958.8 ± 65.02	0.27
VES60-2	3	6.50	60	5.55 ± 1.02	1226.6 ± 176.9	0.34
VES90-1	6	3.25	90	3.51 ± 0.45	710.0 ± 151.0	0.20
VES90-2	6	6.50	90	6.60 ± 0.17	1374.1 ± 285.7	0.38
VMS30-1	3	3.25	30	4.20 ± 0.43	375.7 ± 19.68	0.11
VMS30-2	3	6.50	30	6.71 ± 0.50	1046.5 ± 48.4	0.29
VMS45-1	3	3.25	45	3.33 ± 0.35	998.0 ± 135.8	0.28
VMS45-2	3	6.50	45	6.81 ± 0.63	953.6 ± 151.9	0.27
VMS60-1	3	3.25	60	3.14 ± 0.33	501.9 ± 87.0	0.14
VMS60-2	3	6.50	60	8.15 ± 0.36	1184.3 ± 33.4	0.33
VMS75-1	3	3.25	75	3.36 ± 0.12	798.9 ± 52.0	0.22
VMS75-2	3	6.50	75	6.72 ± 0.41	890.1 ± 68.4	0.25
VMS90-1	3	3.25	90	3.65 ± 0.38	575.8 ± 51.9	0.16
VMS90-2	3	6.50	90	6.72 ± 0.41	1197.9 ± 65.2	0.33

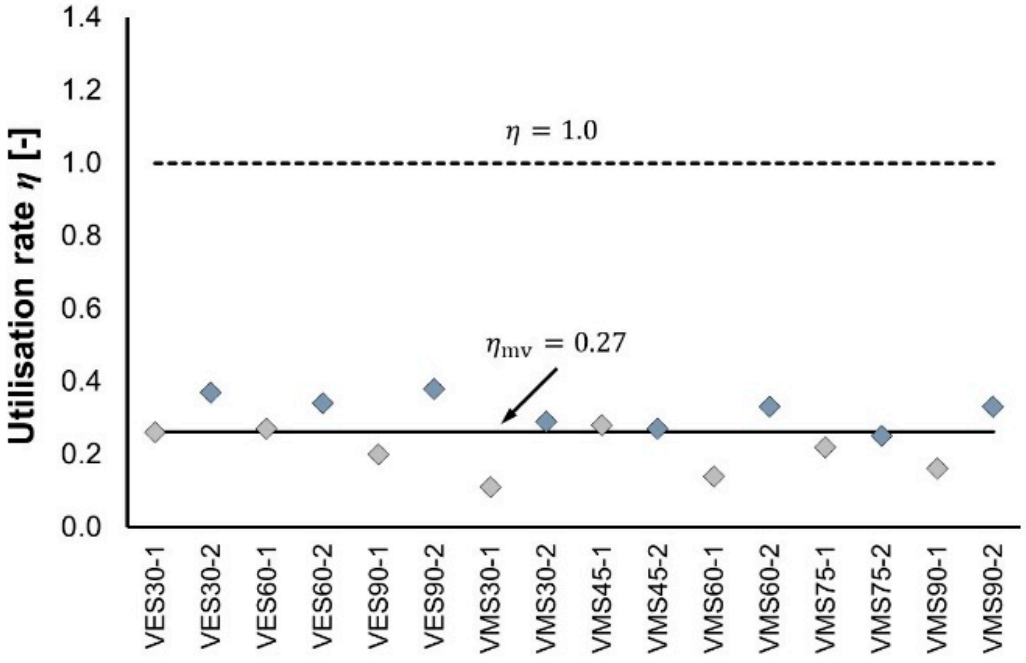

Figure 3. Calculated utilisation rate of pulled out fibres in UHPC under quasi-static loading and mean value.

4.2.2. Cyclic Loading

The test results of the cyclic loaded pullout tests (fibre group pullout tests) were evaluated in an S/N-diagram with related load amplitude and number of cycles to failure. The load amplitude is related to the maximum pullout resistance in Table 2, and no distinction is made with respect to the embedded length. Figure 4 shows the respective S/N-diagram of the pull-out tests.

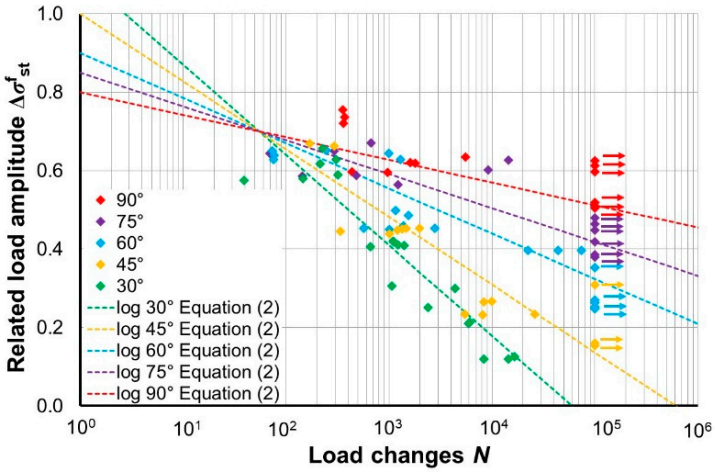

Figure 4. S/N-curves of pullout tests with fibre groups in relation to the fibre orientation.

Figure 4 shows that the fatigue resistance of fibres embedded in UHPC depends significantly on the orientation angle. For each orientation studied, an S/N-line was established using a regression formula given in Equation (2). Detailed background information can be found in [19].

$$\Delta\sigma^{f}_{st} = (0.07 \cdot \ln[\alpha] - 0.34) \cdot \ln N - (0.28 \cdot \ln[\alpha] - 2.05) \quad (2)$$

It can be recorded that the higher the inclination angle of the fibre with respect to the loading direction, the lower the fatigue resistance. The inclination of the fibre also determines the failure mechanism under cyclic loading. Hence, 30° and 45° inclined fibres predominantly exhibit a fibre rupture failure, while 75° and 90° inclined fibres tend to exhibit the bond zone failure. For 60° inclined fibres, both failure mechanisms occur with approximately equal frequency.

Fibre rupture also occurs more frequently at a high embedded depth of approximately 6.50 mm ($= l_f/2$). The reasons for this can be seen in the intensity of the damage to the fibre material, which is caused on the one hand by the orientation and on the other hand by the movement of the fibre as a result of the cyclic loading. As shown in Figure 5, on the left side of the fibre, the load-induced "straightening" is pressing the fibre to the wall of the fibre channel. Due to the cyclic loading, friction occurs between the concrete channel and the fibre material. The friction causes abrasion of the fibre material, which weakens the cross section of the fibre. On the right side of the fibre in Figure 5, additional local bending tensile stresses occur in the fibre because of the "straightening" respectively deflection. The bending stresses enlarge the centric tensile stresses of the fibre, so that locally higher tensile stresses than the measured respectively calculated tensile stresses occur. This leads to a faster degradation, respectively, and lower fatigue resistance.

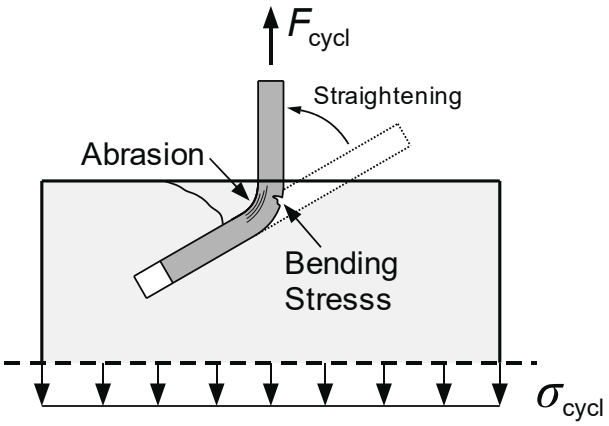

Figure 5. Degradation effects caused by pullout of inclined fibre.

The degradation effects described presumably occur in a certain interaction. Since the stress on the fibre material (abrasion and bending effects) occur at the same place, a relevant damage mechanism cannot be clearly determined. However, it is assumed that the bending effects are the critical type of damage.

5. Interim Conclusions

The experimental investigations based on the fibre pullout tests show that the high-strength micro steel fibre in UHPC is utilized by approximately one third compared to the quasi-static reference tensile strength of the bare fibre (Figure 3). The results of the cyclic tests show, however, that under certain boundary conditions (orientation angle, vibration amplitude), fibre rupture occurs. This means, that even if a sufficient load-bearing reserve can be assumed under quasi-static loading, the fibres could exceed the fatigue strength under cyclic loading.

6. Stress State during Inclined Fibre Pullout

In a straight fibre pullout test, the maximum tensile stress in the fibre can be calculated using Equation (3).

In the inclined pullout test, fibres are bended at the exit point of the fibre channel due to the "straightening" in the loading direction (cf. Figure 6a,b). The level of the bending tensile stress is coupled to the deflection gauge (or mandrel diameter), which is related to the concrete breakout at the fibre exit point. Figure 6c shows qualitatively the stress distribution in the fibre at the exit point from the concrete channel as a result of "straightening".

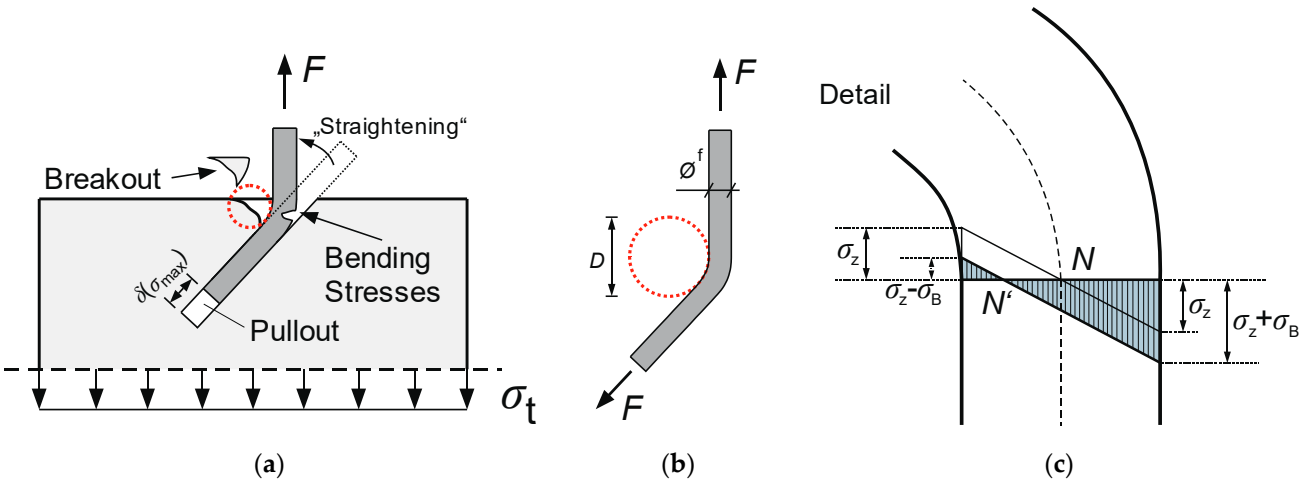

Figure 6. Illustration of bending stress in inclined fibres: (**a**) inclined fibre pullout (**b**) detail of bent fibre (**c**) stress distribution at redirection.

The tensile bending stresses from the deflection σ_B is added to the centric tensile stress σ_Z in the fibre according to Equation (4) with the centric tensile stress calculated using the general form in Equation (3).

$$\sigma_Z = F / A_f \tag{3}$$

$$\sigma_{st}^f = \sigma_Z + \sigma_B \tag{4}$$

The diameter of the fibre $\varnothing^f$ is taken as 0.19 mm according to the manufacturer's data and the investigations in [1]. The additional bending tensile stress σ_B depends on the mandrel diameter D and the Young's modulus E_f of the fibre. With Equation (5), the tensile bending stress is calculated according to Freyer [20]. The background for calculating the bending tensile stress in wires originally comes from Reuleaux [21].

$$\sigma_B = E_f \cdot \frac{\varnothing^f}{D} \tag{5}$$

The Young's modulus of the high strength steel fibre is taken as 169,000 N/mm^2 according to the measurements in [17].

7. Fibre Stresses under Quasi-Static Loading

All quasi-static tests, straight and inclined, show continuous fibre pullout for each test configuration. Accordingly, the tensile stresses in the fibres did not exceed the ultimate tensile strength of the fibre material (f_{st}^{f} = 3575.8 N/mm^2, [1]). Even locally, i.e., at the deflection point, where additional bending stresses occurred, the maximum total tensile stress must have been lower than the ultimate tensile strength.

7.1. Straight Fibre Pullout

The maximum utilization rate according to the test program appeared at test series VES90-2 with $\eta = 0.38$. The value applied to a straight fibre pullout with a measured embedded depth of l_e = 6.60 mm and the assumption that no additional bending stress occurred. Because of the low utilization rate of one third of the fibre's tensile strength, the design of the fibre (geometry, tensile strength) seems to be uneconomical at first. In case the utilization rate of the fibre should be increased, a modification of the fibre design is necessary. For this purpose, the bond model of the embedded fibre must be selected. According to [18], the course of the bond stresses along an embedded fibre can be assumed in good approximation as rigid plastic. With the maximum measured tensile stress from Table 2, the following Equation (6) results for the bond stress.

$$\tau_{st}^{f} = \frac{\sigma_{st,90}^{f} \cdot A_f}{\pi \cdot \varnothing^f \cdot l_e} = \frac{1374.1\,\mathrm{N/mm^2} \cdot \pi \cdot (0.19\,\mathrm{mm}/2)^2}{\pi \cdot 0.19\,\mathrm{mm} \cdot 6.60\,\mathrm{mm}} \approx 10.0\,\mathrm{N/mm^2} \quad (6)$$

Following, the tensile stress $\sigma_{st,90}^{f}$ is replaced by the tensile strength of the fibre material f_{st}^{f}, representing the balance point in regard to fibre rupture. Furthermore, the slenderness $\lambda = l_f/\varnothing^f$ has to be inserted into Equation (6). This is followed by Equation (7).

$$\tau_{st}^{f} = \frac{\sigma_{st,90}^{f} \cdot A_f}{\pi \cdot \varnothing^f \cdot l_e} = \frac{\sigma_{st,90}^{f} \cdot \varnothing^f}{2 \cdot l_f} \rightarrow \eta \cdot f_{st}^{f} = 2 \cdot \tau_{st}^{f} \cdot \lambda = 20 \cdot \lambda \quad (7)$$

With a tensile strength of f_{st}^{f} = 3575.8 N/mm^2, a bond strength of τ_{st}^{f} = 10.0 N/mm^2 and a utilization rate of $\eta = 1.0$ the slenderness of the fibre is maximized to approximately $\lambda = 179$. As the pullout behaviour is accompanied by scatter [17], it is not practical to utilize the full tensile strength of the fibre without a safety margin. Therefore, a reduced utilization rate should be considered. Figure 7 shows possible slendernesses of fibres related to the chosen utilisation rate.

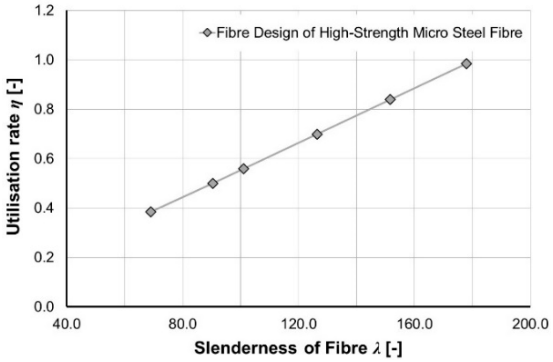

Figure 7. Slenderness of investigated high-strength micro steel fibre in relation to the utilisation rate.

In this context, it must be mentioned that the given slendernesses in Figure 7 is only valid for the investigated fibre type and a straight fibre pullout.

The calculation of the fibre slenderness related to the utilisation rate in Figure 7 depends on a fibre tensile strength of approximately 3576 N/mm^2 that has been measured in [1]. However, the manufacturer states a tensile strength of approximately 2000 N/mm^2.

If the utilisation rate is now correlated to the manufacturer's data, it results in a significantly higher rate and a smaller safety margin (see Equation (8)).

$$\eta = \frac{965.52\ \mathrm{N/mm^2}}{2000\ \mathrm{N/mm^2}} = 0.48 \quad \text{respectively} \quad \gamma = \frac{1}{0.48} = 2.08\ \approx 2.00 \tag{8}$$

7.2. Inclined Fibre Pullout

The additional bending tensile stresses cannot be derived from the measured values. However, they can be calculated with the aid of the formula according to Freyer [20] respectively Reuleaux [21]. The mandrel diameters were determined after the test run, when the inclined fibres were pulled out of the UHPC (Figure 8a). For this purpose, the fibres were carefully removed from the test specimen and examined, respectively, before being measured using a digital microscope. Then, in order to determine the mandrel diameter, circles were iteratively applied to the curvature of the fibres (Figure 8b).

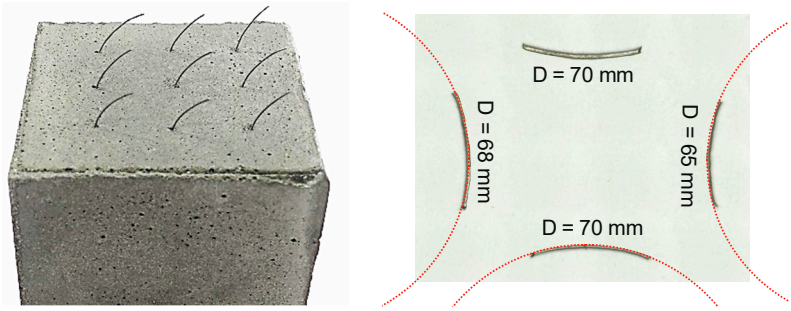

(**a**) (**b**)

Figure 8. Determining the mandrel diameter: (**a**) bent fibres of specimen and (**b**) iteratively applied circles for measuring with digital microscopy.

In addition to the fibers with an orientation of 60°, fibers with an orientation of 30° were also investigated. The measured mandrel diameters are shown in Table 3. The values for 45° and 75° were linearly interpolated and are therefore shown in italics.

Table 3. Calculated mean utilisation rate of pulled out fibres in UHPC under quasi-static loading.

Series	Orientation α	Measured Mandrel Diameter D	Bending Stresses σ_B	Max. (Local) Tensile Stress σ_{st}^f	Utilisation Rate $(\sigma_{st}^f + \sigma_B)/f_{st}^f$
[-]	[°]	[mm]	[N/mm^2]	[N/mm^2]	[-]
VMS30	30	42.0 ± 4.2	764.5	1810.0	0.51
VMS45	*45*	*55.2*	*582.1*	*1580.1*	*0.44*
VMS60	60	68.3 ± 2.4	470.1	1654.4	0.46
VMS75	*75*	*81.5*	*394.2*	*1284.3*	*0.36*

Using the measured mandrel diameters, the bending tensile stresses σ_B were calculated and added to the measured tensile stress from Table 2. It can be seen that the utilization rate of the fibre in the inclined fibre pullout significantly increases from about 0.3 to about 0.5. The utilisation rate in Table 3 is also related to the measured tensile strength of the fibre material [1]. If it is linked to the manufacturer's data, the utilisation rate is even higher (see Equation (9)).

$$\eta = \frac{1810.0\ \mathrm{N/mm^2}}{2000\ \mathrm{N/mm^2}} = 0.91 \quad \text{respectively} \quad \gamma = \frac{1}{0.91} = 1.10\ \approx 1.00 \tag{9}$$

Considering additional bending stresses of fibres and relating them to the manufacturer's tensile strength of the fibre material, the fibre is more or less completely utilized.

To account for the additional bending stresses within the determination of the utilization rate for fibres in UHPFRC, Equation (7) is extended by Equation (5). In addition, the mandrel diameter D is expressed as a function of the orientation angle α following the

same schema like setting up an S/N-curve. A linear relationship according to Equation (10) is assumed between the mandrel diameter D and the orientation angle α in Table 3.

$$D = 0.88 \cdot \alpha + 15.7 \quad \text{für} \quad \alpha < 90^{\circ} \tag{10}$$

The extension of Equation (7) with the additional bending stress in Equation (5), taking into account the linear relationship between the mandrel diameter D and the orientation angle α in Equation (8), yields the utilization rate formulation in Equation (11).

$$\eta \cdot f_{\mathrm{st}}^{\mathrm{f}} = 2 \cdot \tau_{\mathrm{st}}^{\mathrm{f}} \cdot \lambda + E_{\mathrm{f}} \cdot \frac{\varnothing^{\mathrm{f}}}{D} = 2 \cdot \tau_{\mathrm{st}}^{\mathrm{f}} \cdot \lambda + E_{\mathrm{f}} \cdot \frac{\varnothing^{\mathrm{f}}}{0.88 \cdot \alpha + 15.7} \tag{11}$$

8. Fibre Stresses for Cyclic Loading

The experimental results of pullout tests under cyclic tensile loading show that bond failure (fibre pullout) or material failure (fibre rupture) can occur (cf. Section 4.2.2 "Cyclic Loading"). In [1], extensive experimental investigations were carried out with regard to the fatigue strength of bare high-strength micro steel fibres under centric tensile loading. According to [1], and if e.g., a fatigue resistance of $N = 10^6$ load cycles should be maintained, the load amplitude in the bare steel fibre may not exceed $\Delta\sigma_{\mathrm{st}}^{\mathrm{f}}$=178.8 N/mm^2, resulting into a utilization rate of

$$\eta_{\mathrm{fat}}\left(N = 10^6\right) = \frac{\Delta\sigma_{\mathrm{st}}^{\mathrm{f}}}{f_{\mathrm{st}}^{\mathrm{f}}} = \frac{178.8\ \mathrm{N/mm^2}}{3575.8\ \mathrm{N/mm^2}} = 0.05 \tag{12}$$

As mentioned above, in case of an inclined fibre extension a bending tensile stress has to be added to the centric tensile fibre stress. At first, this will not result in a higher amplitude, since the bending tensile stress will be present at top load as well as at bottom load. However, it will increase the load level.

At the current stage of investigation and based on the obtained test results, it appears not feasible to formulate the utilization rate as a function of the fatigue stress, as the load amplitude could apply at different stress levels, and as the load cycles have a considerable influence. Based on current knowledge, a distinction between low-cycle ($N \approx 10^4$) and high-cycle fatigue ($N \geq 10^5$) is feasible in regard to the fibre design.

9. Conclusions and Outlook

The experimental investigations were carried out within the framework of the subproject "Damage processes in ultra-high-performance fibre-reinforced concrete under cyclic tensile loading" with the DFG SPP 2020. The contribution describes a novel approach to select a fibre design for UHPFRC-components considering effects of bending stresses in fibres and cyclic loading. The experimental background has been described in detail by [19], including the consideration of single fibre pullout tests and pullout tests on fibre groups using high-strength micro steel fibres in UHPFRC. The tests were performed under quasi-static and cyclic loading with varying parameters like embedded length and orientation. The stress state during a straight quasi-static fibre pullout is more or less clear. However, inclined fibres show an additional bending stress that occurs at the exit point of the fibre. The additional bending stress can be calculated by the formulae according to [20,21]. Nevertheless, fibres did not rupture during the test execution under quasi-static loading, showing that the fibre design is applicable for UHPFRC. Under certain circumstances (cyclic loading and orientation), fibres embedded in UHPC could also rupture. A local overstraining of the fatigue strength of the fibre material causes the fibre rupture. Fibre rupture in UHPFRC-components could lead to a sudden failure, because the load from the ruptured fibre has to been borne by another fibre. The other fibres are then overstrained again and might also rupture leading to a so-called zipping effect.

Based on the results of the experimental investigations, extensive theoretical considerations were carried out with regard to better methods for fibre design for UHPC. The main findings can be summarized as follows:

- The current fibre design is mainly based on empirical experiences and suitability tests. The effects from a fibre orientation and cyclic loading are not considered appropriately.
- The chosen high-strength micro steel fibres were always pulled out of the UHPC under quasi-static loading. The respective degree of utilization was a maximum of 0.38. On average, the degree of utilization was approximately 0.27. Both values rest upon a measured tensile strength of approximately 3576 N/mm^2. However, the utilisation rate could rise to approximately 0.50, if simplifying respectively without additional testing of the manufacturer's data (2000 N/mm^2).
- At inclined fibres, additional bending stress occurred due to the deflection at the exit point, which must be added to the measured tensile stress in the fibre. The amount of bending tensile stress depends on the fibre orientation. The degree of utilization increased under quasi-static loading to approximately 0.50. If, again, the utilisation rate is related to the manufacturer's specifications, it rises from 0.50 to approximately 1.00. The fibre would then be almost completely utilized. This means that the chosen fibre would have a feasible fibre design under quasi-static loading tailored to the concrete strength and the manufacturer's specifications.
- Under cyclic tensile loading, partial fibre rupture occurred, because the actual load amplitude in the fibre is locally higher due to the additional bending stress resulting from the deflection and reduces the fatigue resistance of inclined oriented fibres. It was not possible to give a quantitative indication, how the fibre is exploited under cyclic tensile loading. The fatigue resistance of the fibre's material and the fatigue bond behaviour are two opposing effects. Probably the above statement on the feasible fibre design, chosen in the own investigations and well-behaving under quasi-static loading, is no longer valid for cyclic loading.

The test results show that, under quasi-static loading, a deterministic fibre design using utilization rates is possible. If the tensile strength of the fibre is obtained in additional tensile tests, certain reserves in relation to the manufacturer's specifications exist and could be used by the given formulas. However, if the UHPC components are stressed by a cyclic tensile loading, partial fibre rupture was observed, especially in the case of inclined fibres. Moreover, a deterministic fibre design, analogous to quasi-static loading, is not possible currently. For this, further fundamental experimental investigations are required. Alternatively, the fatigue resistance of tensile loaded UHPC could be increased by an artificial alignment of the fibres.

Author Contributions: Conceptualization, methodology, software, validation, formal analysis, investigation, resources, data curation, writing—original draft preparation, writing—review and editing, visualization, J.-P.L. and M.E.; supervision, M.E.; project administration, M.E.; funding acquisition, M.E. All authors have read and agreed to the published version of the manuscript.

Funding: German Research Foundation: Priority Program 2020 (DFG number: 353961703).

Institutional Review Board Statement: Not applicable.

Informed Consent Statement: Not applicable.

Acknowledgments: This cooperative research project conducted at iBMB, Division of Concrete Construction, and Institute of Structural Analysis, both at TU Braunschweig, is part of the Priority Program 2020, which is funded by the German Research Foundation (DFG). The authors acknowledge the financial support.

Conflicts of Interest: The authors declare no conflict of interest.

References

1. Lanwer, J.-P.; Empelmann, M. Fundamental Investigations on the Performance of Micro Steel Fibres in Ultra-High-Performance Concrete under Monotonic and Cyclic Tensile Loading. *Appl. Sci.* **2021**, *11*, 9377. [CrossRef]
2. Höper, S. Modelling and Numerical Analysis of the Fibre-Matrix-Bond in UHPFRC Subjected to Tensile Loading. Ph.D. Thesis, Institute for Structural Analysis, TU Braunschweig, Braunschweig, Germany, 18 November 2021. [CrossRef]
3. Fischer, O.; Schramm, N.; Lechner, T. Germany's first application of UHPFRC in railways bridge construction—Part 1: Conception, realisation and practical experiences with a promising material. *Beton Stahlbetonbau* **2018**, *114*, 74–84. [CrossRef]
4. Brühwiler, E.; Friedl, H.; Rupp, C.; Escher, H. Design and construction of a railway bridge in reinforced UHPFRC—World's first UHPFRC bridge on a main railway line. *Beton Stahlbetonbau* **2019**, *114*, 337–345. [CrossRef]
5. Jungwirth, J. Zum Tragverhalten von Zugbeanspruchten Bauteilen aus Ultra-Hochleistungs-Faserbeton. Ph.D. Thesis, École Polytechnique Fédérale De Lausanne, Lausanne, Switzerland, February 2006.
6. Rieger, C. Micro-Fiber Cement Pullout Tests, Uniaxial Tensile Tests and Material Scaling. Ph.D. Thesis, ETH Zurich, Zurich, Switzerland, 2010.
7. Stengel, T. Verbundverhalten und Mechanische Leistungsfähigkeit von Stahlfaser in Ultrahochfestem Beton. Ph.D. Thesis, TU Munich, Munich, Germany, 2013.
8. Wille, K.; Naaman, A.E. Effect of Ultra-High-Performance Concrete on Pullout Behavior of High-Strength Brass-Coated Straight Steel Fibres. *Aci Mater. J.* **2013**, *110*, 451–461.
9. McSwain, A.C.; Berube, K.A.; Cusatis, G.; Landis, E.N. Confinement effects on fiber pullout forces for ultra-high-performance concrete. *Cem. Concr. Compos.* **2018**, *91*, 53–58. [CrossRef]
10. Stürwald, S. *Versuche zum Biegetragverhalten von UHPC mit Kombinierter Bewehrung*; Forschungsbericht, Fachgebiet Massivbau, Fachbereich Bauingenieurwesen, Universität Kassel: Kassel, Germany, 2011.
11. Graybeal, B.A.; Hartman, J.L. Ultra-High Performance Concrete Material Properties. In Proceedings of the 2003 Transportation Research Board Conference, Washington, DC, USA, 12–16 January 2003.
12. Lappa, E.S. High Strength Fibre Reinforced Concrete: Static and Fatigue Behaviour in Bending. Ph.D. Thesis, TU Delft, Delft, The Netherlands, 28 June 2007.
13. Behloul, M.; Chanvillard, G.; Pimienta, P.; Pineaud, A.; Rivillon, P. *Fatigue Flexural Behavior of Pre-Cracked Specimens of Special UHPFRC*; American Concrete Institute: Lansing, MI, USA, 2005; Volume 228, pp. 1253–1268.
14. Cao, Y.Y.Y.; Yu, Q. Effect of inclination angle on hooked end steel fiber pullout behaviour in ultra-high performance concrete. *Compos. Struct.* **2018**, *201*, 151–160. [CrossRef]
15. Schmidt, M.; Fehling, E.; Fröhlich, S.; Thiemicke, J. *Nachhaltiges Bauen mit Ultra-Hochfestem Beton. Sustainable Building with Ultra-High Performance Concrete*; Ergebnisse des Schwerpunktprogrammes 1182 gefördert durch die Deutsche Forschungsgemeinschaft (DFG); Schriftenreihe Baustoffe und Massivbau, Heft 22; Kassel University Press: Kassel, Germany, 2014.
16. Lanwer, J.; Oettel, V.; Empelmann, M.; Höper, S.; Kowalsky, U.; Dinkler, D. Bond behavior of micro steel fibers embedded in ultra-high performance concrete subjected to monotonic and cyclic loading. *Struct. Concr.* **2019**, *20*, 1243–1253. [CrossRef]
17. Oettel, V.; Lanwer, J.-P.; Empelmann, M. Pullout behaviour of micro steel fibres of UHPC under monotonic and cyclic loading. *Bauingenieur* **2021**, *96*, 1–10. [CrossRef]
18. Schmidt, M.; Bunje, K.; Fehling, E.; Teichmann, T. Brückenfamilie aus Ultra-Hochfestem Beton in Niestetal und Kassel. *Beton Stahlbetonbau* **2006**, *101*, 198–204. [CrossRef]
19. Lanwer, J.-P.; Höper, S.; Gietz, L.; Kowalsky, U.; Empelmann, M.; Dinkler, D. Fundamental Investigations of Bond Behaviour of High-Strength Micro Steel Fibres in Ultra-High Performance Concrete under Cyclic Tensile Loading. *Materials* **2021**, *15*, 120. [CrossRef] [PubMed]
20. Freyer, K. Wire Ropes Under Bending and Tensile Stresses. In *Wire Ropes*; Springer: Berlin/Heidelberg, Germany, 2007. [CrossRef]
21. Reuleaux, F. *Der Konstrukteur*; 4. Überarbeitete und Erweiterte Auflage; Ernst & Sohn: Braunschweig, Germany, 1882–1889.